


Study on intercalation in layered structure of halloysite nanotubes (HNTs)

Zhi-Lin Cheng , Bao-Chong Cao, Zan Liu

College of Chemistry and Chemical Engineering, Yangzhou University, 225002, People's Republic of China

✉ E-mail: zlcheng224@126.com

Published in Micro & Nano Letters; Received on 11th October 2018; Revised on 1st February 2019; Accepted on 11th February 2019

The organic-intercalated clay composites have aroused attractable interest due to their tremendous application in industry. As a new type of the layered-structure material, halloysite nanotubes (HNTs) were employed to explore the intercalation relationship between the interlayer property and intercalating agents, which were more significant for the potential application. For this purpose, this work systematically studied the intercalation behaviours of dimethyl sulphoxide, potassium acetate, *N*-methylformamide, methanol, and acrylamide in the layered-structure HNTs, respectively. The organics-intercalated HNT composites were determined by a series of characterisations.

1. Introduction: In recent years, organic/inorganic intercalated composites have received more attention due to their low cost and remarkable improvement in mechanical, thermal, optical and physicochemical properties compared with that of unmodified composites [1]. They can be widely used in petrochemical, biological engineering, ceramics, sewage treatment, packaging materials, fire-retardant materials and other fields [2–4]. Additionally, clays could be used as alternative adsorbents for the removal of heavy metals from waste water because their adsorption capacities were significantly improved after modification [5]. Sarier *et al.* [6] intercalated low molecular weight polyethylene glycol into Na-montmorillonite in the montmorillonite suspension. Yang *et al.* [7] reported a low-cost and environmental friendly adsorbing material for formaldehyde, which was made from L-alanine-intercalated kaolinite.

Halloysite nanotubes (HNTs) as a natural aluminosilicate mineral ($\text{Al}_2(\text{OH})_4\text{Si}_2\text{O}_5 \cdot n\text{H}_2\text{O}$, $n=0$ or 2) have a high aspect ratio with 0.1–2 μm in length and 40–70 nm in outer diameters. Furthermore, HNTs possess a distinctive crimped layered structure, the interlayer spacing of which is about 10 Å, and attain 7 Å when heated under mild conditions. Owing to low cost and abundant availability, HNTs were broadly applied in photocatalysts [8], corrosion inhibitors [9], polymer nanocomposites [10], drug delivery [11], and adsorbents [12]. The intercalation of inorganic and organic species in the interlayer spaces of halloysite without destruction of the layered structure has recently begun to gain increasing attention due to the potential industrial applications in polymer nanocomposites. Nowadays, organic-intercalated montmorillonite composites have been used widely in the industry because montmorillonite has exchangeable cations within its interlayer space. However, HNTs have only tiny exchangeable cation located in the interlayer, and therefore there are hardly exchangeable cations replaced by the intercalating agents. Actually, it has been proved that the micromolecules with intense polarity might be intercalated smoothly into the layered structure of HNTs [13–24]. For instance, Adamczyk *et al.* [20] achieved the interlayer spacing of HNTs from 7.1 to 10.3 Å using formamide intercalation, and the intercalation complex was stable below 60°C. Mahreza *et al.* [21] studied dimethyl sulphoxide (DMSO)-intercalated HNTs with an interlayer spacing of 11.2 Å, which could be used as an adsorbent to adsorb crystal violet in aqueous solution. Horváth *et al.* [22] reported that the hydrazine hydrate moieties were intercalated directly into the interlayer of HNTs through forming the hydrogen bonds between water and the surface hydroxyl groups into the interlayer. Nicolini *et al.* [23] studied the urea-intercalated HNTs with the interlayer spacing of 3.3 Å. Cheng *et al.* [24] studied the molecular structure of the potassium acetate-intercalated HNTs and demonstrated the presence of the

structural change of HNTs after intercalation. However, few research studies focused on revealing the intercalating relationship between the properties of the intercalating molecular and layered structure of HNTs. Inspired by this reason, this Letter studies the intercalation behaviours of five types of molecules with different properties in the layered structure of HNTs. The structure of the resulting organic/inorganic intercalated composites was determined by using a series of characterisations. The mechanism of the intercalation was proposed.

2. Experimental: Before using, raw HNTs (HNTs-10 Å) were dried at 100°C for overnight, obtaining HNTs-7 Å. The intercalation illustration was displayed in Fig. 1. DMSO, *N*-methylformamide (NMF), and potassium acetate (KAc) could be directly intercalated into the layered structure of HNTs, denoted HNTs-DMSO, HNTs-KAc, and HNTs-NMF, respectively. HNTs-DMSO: the intercalation of DMSO into HNTs was carried out at 60°C for 24 h by stirring the suspension of the dried HNTs (5 g), DMSO (60 ml) and H_2O (6 ml). The intercalated samples were washed three times with anhydrous ethanol and dried at 60°C for 48 h. HNTs-KAc: the mixture of HNTs (5 g), CH_3COOK (4 g) and deionised water (1 ml) was put in a mortar, and then sufficiently grind to make them a homogeneous mixture. The mixture was placed at room temperature for 24 h and then added 50 ml anhydrous ethanol with stirring. The sample was centrifuged and dried at 60°C for 48 h. HNTs-NMF: NMF intercalated HNTs composite was obtained at room temperature for 72 h by stirring the suspension of the dry HNTs (5 g), NMF (50 ml), and H_2O (5 ml). The intercalated sample was washed three times with anhydrous ethanol to remove the excess NMF, followed by drying at 60°C for 48 h. However, the experiments found that methanol (MeOH) and acrylamide (AM) could not be directly intercalated into the layered structure of HNTs. Accordingly, their composites were achieved through the substitution method using HNTs-DMSO or HNTs-KAc as precursors, denoted HNTs-MeOH and HNTs-AM, respectively. HNTs-Me: the intercalation of MeOH intercalated HNTs was carried out at room temperature for 7 days by stirring the suspension of the HNTs-DMSO (5 g) and MeOH (100 ml). During preparation, MeOH (100 ml) needed to be replaced every day. The intercalated sample was washed three times with MeOH and dried at 40°C for 48 h. HNTs-AM: 10 g of AM was dissolved in 40 ml anhydrous ethanol, and 2 g of HNTs-KAc sample was added. The suspension was stirred for 24 h at 60°C. The resulting sample was centrifuged and washed by anhydrous ethanol to remove KAc and excessive AM. The intercalation rate (IR) was calculated from X-ray



Fig. 1 Schematic illustration of HNTs intercalated with different intercalating agents

diffraction (XRD) measurement according to the following equation:

$$IR = \frac{I_1}{I_0 + I_1} \times 100\%,$$

where I_1 refers to the first reflection intensity of the new phase and I_0 is the residuary (0 0 1) reflection intensity in the compound.

3. Results and discussion: Fig. 2 shows the XRD patterns of raw HNTs, 7 Å HNTs, and different organic-intercalated HNTs composites. For HNTs, the (001) reflection plane corresponds to the first basal reflection. A feature peak at $2\theta = 23.5^\circ$ is associated with the (110) reflection plane, which is assigned to the turbostratic stacking of the layered structure of HNTs [8]. The diffraction peaks in (002), (003), and (200) reflection planes are consistent with HNTs (indexed by JCPDS Card No. 74-1022). The raw HNTs (HNTs-10 Å) have two diffraction peaks at 8.9° and a broad peak at 11.5° . As shown in Fig. 2b, after drying, the basal spacing changes from 10 to 7 Å because of the removal of the interlayer water of HNTs-10 Å, accessing so-called HNTs-7 Å. As for HNTs-DMSO, HNTs-KAc and HNTs-NMF composites (Figs. 2c–e), the basal spacing enlarges from 0.72 nm of HNTs-7 Å to 1.12 nm (HNTs-DMSO), 1.42 nm (HNTs-KAc) and 1.08 nm (HNTs-NMF) arose from the intercalation, indicating that DMSO, KAc, and NMF have been successfully intercalated into the layered structure of HNTs by the first-step method. In addition, the (0 0 1) peak of HNTs was not observed in patterns (Figs. 2c and e), suggesting that the IR of HNTs-NMF and HNTs-DMSO both are ~100%. Surprisingly, it is found that a smaller-sized MeOH cannot be directly intercalated into the layered structure of HNTs in the experiment, and its intercalation need be achieved by the substitution method based on the HNTs-DMSO as a precursor. After substitution, the basal spacing

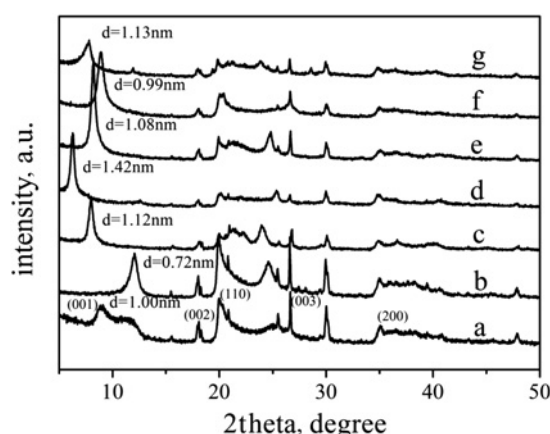


Fig. 2 XRD patterns of
a HNTs-10 Å
b HNTs-7 Å
c HNTs-DMSO
d HNTs-KAc
e HNTs-NMF
f HNTs-Me
g HNTs-AM

of HNTs-DMSO varies from 1.12 nm decreasing to 0.99 nm. Moreover, the (0 0 1) diffraction peak of HNTs-DMSO disappears, indicating that MeOH was successfully replaced by DMSO in the layered structure of HNTs. Similarly, AM also cannot be directly intercalated into the layered structure of HNTs, thus introducing it in the layered structure by replacing KAc with substitution intercalation (Fig. 2g). The basal spacing of the HNTs-AM decreases from 1.42 to 1.11 nm, suggesting the successful intercalation by the substitution method.

Fig. 3 gives the Fourier transform-infrared (FTIR) spectra of HNTs-7 Å, HNTs-10 Å, and different organic-intercalated HNTs composites. For HNTs, the adsorption bands at 3694 and 3620 cm^{-1} are ascribed to the stretching vibration of the surface and inner hydroxyl, respectively. The adsorption bands at 1091 and 1030 cm^{-1} are ascribed to the Si–O stretching vibration, and the adsorption bands at 1033 and 912 cm^{-1} are attributed to the stretching vibrations of Si–O–Si and bending modes of Al–O–H. The adsorption band at 754 cm^{-1} is caused by the vertical stretching vibration of Si–O. The adsorption bands at 542 and 470 cm^{-1} are assigned to the bending vibrations of Al–O–Al and Si–O–Si, respectively [25, 26]. After being dried, the FTIR spectrum of HNTs-7 Å exhibits no change with HNTs-10 Å. After being intercalated with DMSO (Fig. 3c), the disappearance of the adsorption band at 3694 cm^{-1} and the appearance of 3700 and 3664 cm^{-1} , indicating that DMSO is liable to have interacted with the inner surface hydroxyls of HNTs through hydrogen bonds with the S=O groups. As expected, the adsorption band at 3620 cm^{-1} has no significant influence since the corresponding OH groups are located between the tetrahedral and octahedral sheets, which are not disturbed by the intercalation process. The adsorption band at 3496 cm^{-1} is due to the hydrogen bond formation between hydrogen in water and lone pairs of electrons of the sulphur atom in DMSO. The adsorption bands at 3022 and 2937 cm^{-1} are attributed to the antisymmetric and symmetric stretching vibrations of the C–H in the methyl group, indicating that DMSO is intercalated in the layered structure of HNTs via an interaction with the inner surface hydroxyls of HNTs. The adsorption bands at 1436, 1407, 1376 and 1319 cm^{-1} are attributed to the bending vibration of CH_3 . This demonstrates that DMSO is located in the layered structure of HNTs [8]. As shown in Fig. 3d, the absorption bands at 1569 and 1418 cm^{-1} are attributed to the antisymmetric and symmetric stretching vibrations of CH_3COO^- . The absorption band at

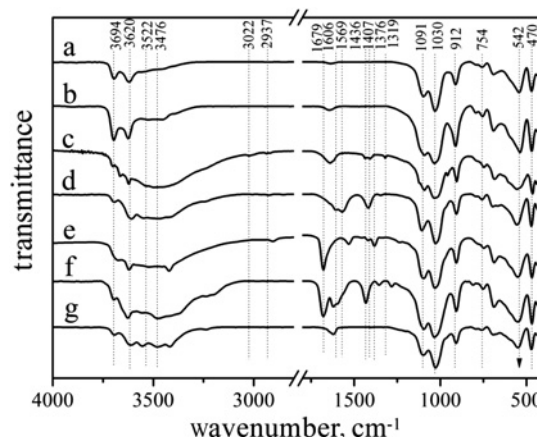


Fig. 3 FTIR spectra of
a HNTs-10 Å
b HNTs-7 Å
c HNTs-DMSO
d HNTs-KAc
e HNTs-NMF
f HNTs-Me
g HNTs-AM

1606 cm^{-1} resulted from the superposition of the antisymmetric stretching vibration of CH_3COO^- and the bending vibration of H_2O . The absorption bands at 3696 and 3622 cm^{-1} disappear, whereas the adsorption bands at 3693 and 3608 cm^{-1} appear. These results indicate that the new hydrogen bond is created between the inner surface hydroxyl of HNTs and KAc. For HNTs-NMF (Fig. 3e), the absorption band at 3620 cm^{-1} has no change. However, the absorption band at 3696 cm^{-1} disappear and two absorption bands at 1679 and 3522 cm^{-1} attributed to C=O and NH in NMF appear, indicating that NH and C=O attach to Si-O and Al-O-H in HNTs by forming a hydrogen bond, thus demonstrating NMF is intercalated into the layered structure of HNTs. In the FTIR spectrum of HNTs-Me composites, the absorption bands at 3022 and 2937 cm^{-1} disappear while appearing the absorption bands at 3554 cm^{-1} caused from the stretching vibration of -OH in MeOH. The absorption bands at 1436, 1407, 1376, and 1319 cm^{-1} attributed to the bending vibration of CH_3 also disappear, indicating that MeOH has successfully replaced DMSO in the layered structure of HNTs by the substitution method. In the FTIR spectrum of HNTs-AM composites (Fig. 3g), the absorption bands at 3693 and 3608 cm^{-1} are not observed. The new absorption bands appear at 3626, 3555, and 3476 cm^{-1} due to hydrogen bonding between hydroxyls of HNTs and AM. The absorption bands at 1679, 1620 and 1432 cm^{-1} are attributed to the stretching vibration of C=C, deformation vibration of NH and deformation vibration of CH_2 , respectively. Also, the absorption bands at 1569 and 1418 cm^{-1} attributed to antisymmetric and symmetric stretching vibration of CH_3COO^- disappear, indicating that AM was successfully intercalated into the layered structure of HNTs by the substitution method [27].

The thermogravimetry (TG) and derivative thermogravimetry (DTG) curves of HNTs and different organic-intercalated HNTs composites are shown in Fig. 4. As to HNTs, 4.15% mass loss corresponding to adsorbed water is observed at about 100°C and 12.86% mass loss of dehydroxylation takes place at 482°C [12]. The HNTs-DMSO composite has three mass losses, which correspond to 12.77% mass loss of adsorbed water at 75°C, 12.73% mass loss of DMSO decomposition at 180°C and 9.07% mass loss of

strong dehydroxylation at 486°C, respectively. It can be found that the dehydroxylation rate drops due to the intercalation of DMSO. The HNTs-KAc composite has three main mass losses corresponding to adsorbed water (3.29% mass loss) at 81°C, KAc decomposition (18.60% mass loss) at 365°C and weak dehydroxylation at about 480°C, respectively. The HNTs-NMF composite has four obvious mass losses associated with adsorbed water (10.75% mass loss) at 81°C, NMF decomposition (12.73% mass loss) at 164°C, weak new bonding (3.16% mass loss) at 362°C and strong dehydroxylation (9.55% mass loss) at 482°C, respectively. The HNTs-Me composite presents two notable mass losses corresponding to adsorbed water (3.08% mass loss) at about 100°C and dehydroxylation (9.55% mass loss) at 482°C, respectively. This indicates that MeOH in the layered structure of HNTs is easily volatile at low temperature. The HNTs-AM composite has three main mass losses assigned to adsorbed water (4.30% mass loss) at 120°C, AM decomposition (2.70% mass loss) at 344°C and weak dehydroxylation (8.21% mass loss) at 456°C, respectively. More importantly, after intercalation of those organic molecules (Fig. 5), the feature of the tubular structure of HNTs retains very well.

To be similar to kaolinite [28], it is well known that only those organic molecules with high dipole moment that is prone to form stronger hydrogen bond are conducive to be effectively intercalated into the layered structure of HNTs. As shown in Table 1, DMSO has a high dipole moment (3.96), and its molecular size is 0.39 nm which is much smaller than that of HNTs. After DMSO intercalation, the basal spacing enlarges from 0.72 nm of HNTs to 1.12 nm, supposing that the sulphoxide group (S=O) of DMSO forms a hydrogen bond with the inner surface hydroxyl groups (Al-OH) and the methyl group prefers to face the Si-O surface. With KAc intercalation, the water molecule plays an important role in the intercalation process. Acetate with a molecular size of 0.25 nm belongs to an ionic compound, and is of the strongest dipolar property among these molecules. So, it is easily intercalated into the layered structure of HNTs due to the existence of the electric field. NMF as the amide-based guest molecular structure is a proton donor and a receptor with C=O that forms a hydrogen bond with the inner surface hydroxyl group (Al-OH) bond while

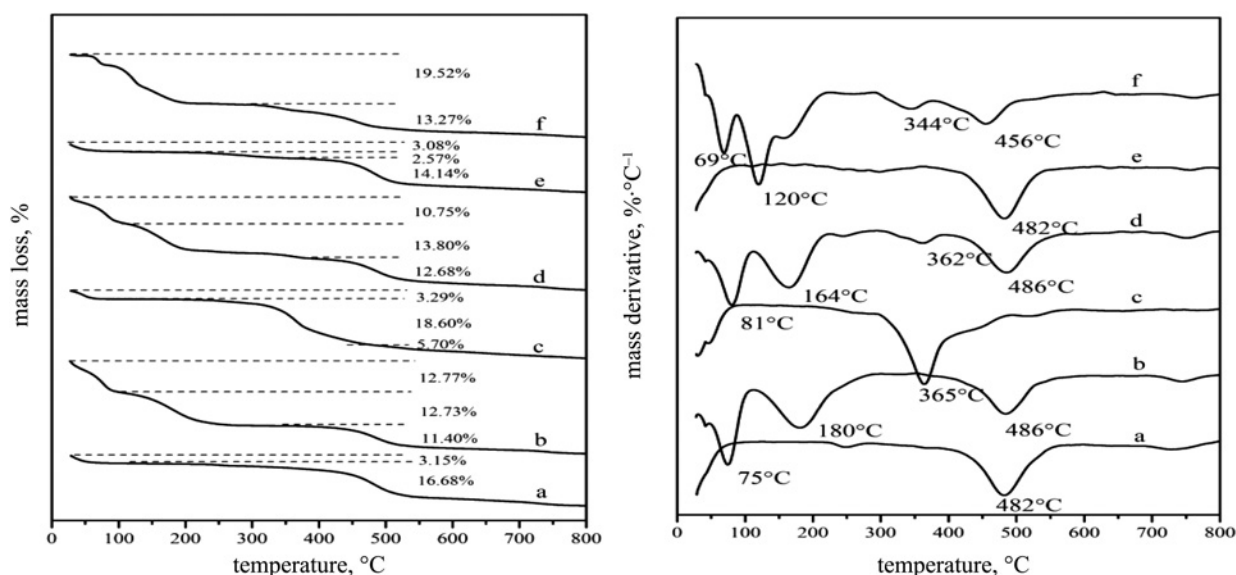


Fig. 4 TG-DTG curves of
a HNTs
b HNTs-DMSO
c HNTs-KAc
d HNTs-NMF
e HNTs-Me
f HNTs-AM

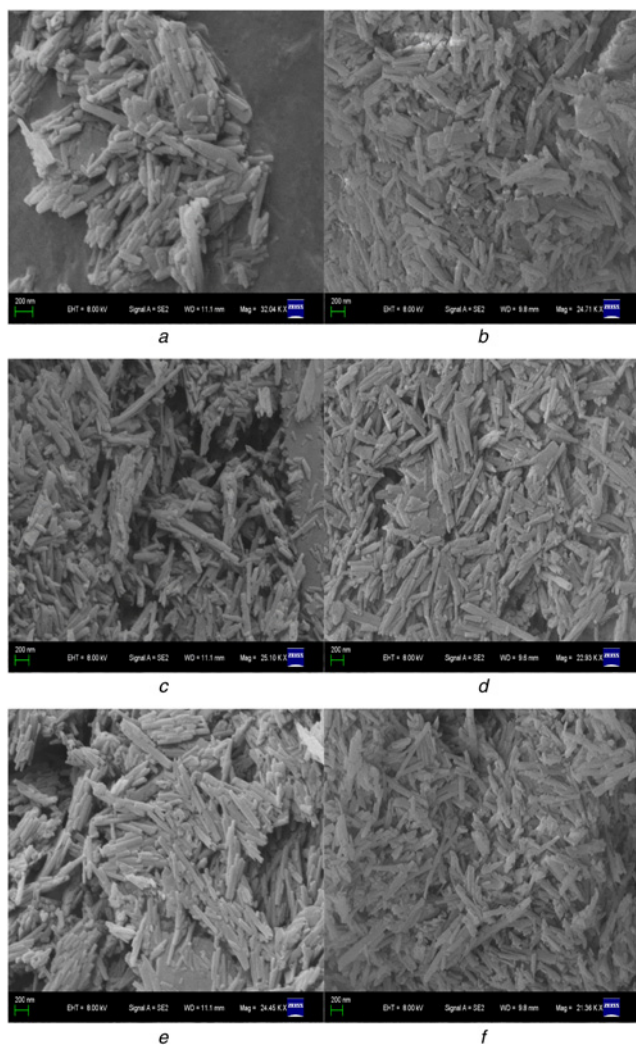


Fig. 5 Scanning electron microscopy photos of
a HNTs
b HNTs-DMSO
c HNTs-KAc
d HNTs-NMF
e HNTs-Me
f HNTs-AM

Table 1 Dipole moment, molecule dimension and d value of intercalating compound

Composites	Intercalation molecules dipole moment (D)	Intercalation molecules dimension, nm	d_{001} , nm	Δd , nm
HNTs-10 Å	—	—	1.00	—
HNTs-7 Å	—	—	0.72	—
HNTs-DMSO	3.96	0.39	1.12	0.40
HNTs-KAc	— ^a	0.38	1.42	0.70
HNTs-NMF	3.83	0.36	1.08	0.36
HNTs-MeOH	1.70	0.43	0.99	0.27
HNTs-AM	3.44	0.40	1.13	0.41

^aNot found.

—NH₂ forms a hydrogen bond with siloxy groups. Since MeOH and AM have a smaller dipole moment and larger molecule dimension than those of DMSO and NMF, they are difficult to intercalate in the layered structure of HNTs directly, thus adopting the substitution intercalation.

4. Conclusion: Five types of intercalating agents were successfully intercalated in the layered structure of HNTs. The characterisations showed that DMSO, NMF, and KAc could be directly intercalated in the layered structure of HNTs, whereas MeOH and AM needed through the substitution method that fulfilled intercalation by direct intercalation. Ultimately, the probable intercalating mechanism based on the layered structure of HNTs was discussed.

5. Acknowledgment: This work was funded by the Talent Introduction Fund of Yangzhou University (2012), Zhenjiang High Technology Research Institute of Yangzhou University (2017), Key Research Project-Industry Foresight and General Key Technology of Yangzhou (grant no. YZ2015020), Innovative Talent Program of Green Yang Golden Phoenix (grant no. yzlyjfh2015CX073), Yangzhou Social Development Project (grant no. YZ2016072) and Six Talent Peaks Project of Jiangsu Province (grant no. 2014-XCL-013). The data of this Letter originated from the Test Center of Yangzhou University.

6 References

- [1] Xia H., Zhang S.H.: 'Synthesis, characterization and mechanism of benzamide intercalated kaolinite by replacement method', *Appl. Mech. Mater.*, 2013, **420**, pp. 222–229
- [2] Wu P.X., Li W., Zhu Y.J., *ET AL.*: 'The protective effect of layered double hydroxide against damage to DNA induced by heavy metals', *Appl. Clay Sci.*, 2014, **100**, (10), pp. 76–83
- [3] Ludueña L.N., Vázquez A., Alvarez V.A.: 'Effect of the type of clay organo – modifier on the morphology, thermal/mechanical/impact/barrier properties and biodegradation in soil of polycaprolactone/clay nanocomposites', *J. Appl. Polym. Sci.*, 2013, **128**, (5), pp. 2648–2657
- [4] Zhu X., Yan C., Chen J.: 'Application of urea-intercalated kaolinite for paper coating', *Appl. Clay Sci.*, 2012, **55**, (7), pp. 114–119
- [5] Tepmatee P., Siriphannon P.: 'Facile preparation of copper impregnated aluminum pillared montmorillonite: nanoclays for wastewater treatment', *Bull. Polish Acad. Sci. Tech. Sci.*, 2016, **64**, (3), pp. 553–560
- [6] Sarier N., Onder E.: 'Organic modification of montmorillonite with low molecular weight polyethylene glycols and its use in polyurethane nanocomposite foams', *Thermochim. Acta*, 2010, **510**, (1), pp. 113–121
- [7] Yang H., Sun X., Liu S.X., *ET AL.*: 'Low – cost and environmental – friendly kaolinite – intercalated hybrid material showing fast formaldehyde adsorbing behavior', *ChemistrySelect*, 2016, **1**, (10), pp. 2181–2187
- [8] Papoulis D., Komarneni S., Nikolopoulou A., *ET AL.*: 'Palygorskite- and halloysite-TiO₂, nanocomposites: synthesis and photocatalytic activity', *Appl. Clay Sci.*, 2010, **50**, (1), pp. 118–124
- [9] Jafari A.H., Hosseini S.M.A., Jamalizadeh E.: 'Investigation of smart nanocapsules containing inhibitors for corrosion protection of copper', *Electrochim. Acta*, 2010, **55**, (28), pp. 9004–9009
- [10] Carli L.N., Daitx T.S., Soares G.V., *ET AL.*: 'The effects of silane coupling agents on the properties of PHBV/halloysite nanocomposites', *Appl. Clay Sci.*, 2014, **87**, (4), pp. 311–319
- [11] Rao K.M., Nagappan S., Seo D.J., *ET AL.*: 'pH sensitive halloysite-sodium hyaluronate/poly(hydroxyethyl methacrylate) nanocomposites for colon cancer drug delivery', *Appl. Clay Sci.*, 2014, **97–98**, (2014), pp. 33–42
- [12] Errais E., Duplay J., Elhabiri M., *ET AL.*: 'Anionic RR120 dye adsorption onto raw clay: surface properties and adsorption mechanism', *Colloids Surf. A, Physicochem. Eng. Aspects*, 2012, **403**, (403), pp. 69–78
- [13] Costanzo P.M.: 'Ordered halloysite: dimethyl sulfoxide intercalate', *Clays Clay Miner.*, 1986, **34**, (1), pp. 105–107
- [14] Horváth E., Kristóf J., Kurdi R., *ET AL.*: 'Study of urea intercalation into halloysite by thermos analytical and spectroscopic techniques', *J. Therm. Anal. Calorim.*, 2011, **105**, (1), pp. 53–59
- [15] Mellouk S., Belhakem A., Marouf-Khelifa K., *ET AL.*: 'Cu(II) adsorption by halloysites intercalated with sodium acetate', *J. Colloid Interface Sci.*, 2011, **360**, (2), pp. 716–724
- [16] Frost R.L., Kristof J., Horvath E., *ET AL.*: 'Rehydration and phase changes of potassium acetate-intercalated halloysite at 298 K', *J. Colloid Interface Sci.*, 2000, **226**, (2), pp. 318–327

- [17] Frost R.L., Kristof J., Mako E., *ET AL.*: 'Modification of the hydroxyl surface in potassium-acetate-intercalated kaolinite between 25 and 300°C', *Langmuir*, 2000, **16**, (19), pp. 1735–1743
- [18] Mako E., Kovacs A., Horvath E., *ET AL.*: 'Kaolinite-potassium acetate and halloysite-potassium acetate complexes prepared by mechanochemical, solution and homogenization techniques: a comparative study', *Clay Miner.*, 2014, **49**, (3), pp. 457–471(15)
- [19] Churchman G.J., Theng B.K.G.: 'Interactions of halloysites with amides: mineralogical factors affecting complex formation', *Electron. Commun. Japan*, 1984, **63**, (2), pp. 99–106
- [20] Adamczyk M., Rok M., Wolny A., *ET AL.*: 'Dielectric properties of halloysite and halloysite-formamide intercalate', *J. Appl. Phys.*, 2014, **115**, (2), pp. 024101–024101-5
- [21] Mahreza N., Bendeniaa S., Marouf-Khelifaa K., *ET AL.*: 'Improving of the adsorption capacity of halloysite nanotubes intercalated with dimethyl sulfoxide', *Compos. Interfaces*, 2015, **22**, (6), pp. 1–15
- [22] Horváth E., Kristóf J., Frost R.L., *ET AL.*: 'Hydrazine-hydrate intercalated halloysite under controlled-rate thermal analysis conditions', *J. Therm. Anal. Calorim.*, 2003, **71**, (3), pp. 707–714
- [23] Nicolini K.P., Fukamachi C.R., Wypych F., *ET AL.*: 'Dehydrated halloysite intercalated mechanochemically with urea: thermal behavior and structural aspects', *J. Colloid Interface Sci.*, 2009, **338**, (2), pp. 474–479
- [24] Cheng H., Liu Q., Yang J., *ET AL.*: 'Infrared spectroscopic study of halloysite-potassium acetate intercalation complex', *J. Mol. Struct.*, 2011, **990**, (1–3), pp. 21–25
- [25] Luo P., Zhao Y.F., Zhang B., *ET AL.*: 'Study on the adsorption of neutral red from aqueous solution onto halloysite nanotubes', *Water Res.*, 2010, **44**, (5), pp. 1489–1497
- [26] Wang L., Chen J.L., Ge L., *ET AL.*: 'Halloysite-nanotube-supported Ru nanoparticles for ammonia catalytic decomposition to produce Cox-free hydrogen', *Energy Fuels*, 2011, **25**, (8), pp. 3408–3416
- [27] Sugahara Y., Satokawa S., Kuroda K., *ET AL.*: 'Preparation of a kaolinite-polyacrylamide intercalation compound', *Clays Clay Miner.*, 1990, **38**, (2), pp. 137–143
- [28] Cheng H., Liu Q., Yang J., *ET AL.*: 'Influencing factors on kaolinite–potassium acetate intercalation complexes', *Appl. Clay Sci.*, 2010, **50**, (4), pp. 476–480